

Received May 25, 2019, accepted July 8, 2019, date of publication July 12, 2019, date of current version August 1, 2019.

Digital Object Identifier 10.1109/ACCESS.2019.2928440

A Novel Model Predictive Control via Optimized Vector Selection Method for Common-Mode Voltage Reduction of Three-Phase Inverters

TAO JIN^{1,2}, (Senior Member, IEEE), JINTAO GUO^{1,2},
MOHAMED A. MOHAMED^{2,3}, (Member, IEEE),
AND MENGQI WANG⁴, (Member, IEEE)

¹Fujian Key Laboratory of New Energy Generation and Power Conversion, Fuzhou 350116, China

²Department of Electrical Engineering, Fuzhou University, Fuzhou 350116, China

³Electrical Engineering Department, Faculty of Engineering, Minia University, Minia 61519, Egypt

⁴Department of Electrical and Computer Engineering, College of Engineering and Computer Science, University of Michigan–Dearborn, Dearborn, MI 48128, USA

Corresponding authors: Tao Jin (jintly@fzu.edu.cn) and Mengqi Wang (mengqi@umich.edu)

This work was supported by the National Natural Science Foundation of China under Grant 51807031.

ABSTRACT In this paper, a novel model predictive control (MPC) via a double vector optimized selection method is proposed. The main idea of this method is for decreasing the high common-mode voltage of two-level inverter under balance situation, improve the tracking performance of the output current and decrease the high output current harmonic distortion rate. To solve the problem of increasing the value of total harmonic distortion (THD) due to the reduction of the available voltage vector, this method controls two voltage vectors in each sampling period for getting a better tracking performance of the output current. Simultaneously, compared with the adding virtual vector MPC method, which results in excessive switching losses, the proposed method defining the selection range of the second voltage vector. Only two voltage vectors adjacent to the first voltage vector can be selected so that the switching frequency can be greatly reduced. An experimental control platform based on Simulink-Real-Time system is presented for the further verification of the effectiveness of the proposed control method. The simulation and experimental results showed that the proposed method could effectively reduce the output common-mode voltage of the inverter. Simultaneously, the THD value and the switching loss are greatly reduced.

INDEX TERMS Model predictive control, common-mode voltage, double vector controlling, three-phase two level inverter.

I. INTRODUCTION

Nowadays, with the tremendous development of the power electronics technology, power electronics such as power converters, high-performance adjustable speed transmissions are widely used in AC transmission, active filtering, energy generation etc. [1]. Furthermore, along with the development of power electronics applications in the field of high voltage, high capacity, high power density and high switching frequency, the inverter output common-mode voltage has become more and more serious. The common-mode voltage not only causes electromagnetic interference, but also harms the normal operation of nearby electronic equipment [2]–[6]. What's more, the high common-mode voltage causes higher

motor shaft voltage and current, which affects its life span [5]. Therefore, it is significant to study the control technology for reducing the inverter output common-mode voltage.

Several effective techniques have been proposed in the literatures for reducing and eliminating the inverter output common-mode voltage. At present, the methods that reduce the output common-mode voltage can be sorted into hardware modulation method and software modulation method [7]. In the context of hardware modulation methods, Yang *et al.* [2], Tallam *et al.* [8] proposed control methods by adding additional device such as isolation transformer, passive filtering, active filtering, etc. These control methods however, enlarge the total size, increase the complexity and disturb the dynamics of system. Renge and Suryawanshi [9], Akagi and Tamura [10], Qin *et al.* [11] the authors proposed a method that uses the topology of four-leg converter and

The associate editor coordinating the review of this manuscript and approving it for publication was Rongni Yang.

quasi-z-source three-level T-type inverter to reduce the output common-mode voltage of inverter. Through these methods, the inverter output common-mode voltage can be reduced, however it is complicated to design the hardware through this method, also increase the system size and cost [12]. In addition, improving the control strategy algorithm by software method is another conventional way for reducing the inverter output common-mode voltage. Sinusoidal pulse width modulation (PWM) is one of the most utilized conventional modulation techniques for inverters control and common-mode voltage reduction [13], [14]. Although the improved PWM control strategy does not require additional investment, the design of the PWM model and the implementation of such methods are more complex [15]. In contrast, because of its advantages of convenient implementation, flexible control, and no need for a PWM model, the model predictive control (MPC) has been widely applied in the field of power electronic control in recent years [17].

The MPC was first used in industrial process control, which has great advantages in dealing with complex constrained optimization problems of nonlinear systems [16], [17]. In [18], in contrast to conventional MPC, the author proposed a MPC method that discards the zero voltage vector directly. In this method, the inverter output common-mode voltage can be decreased without making major changes to the conventional MPC. However, this method for reducing the output common-mode voltage will greatly disturb the load current tracking performance, which affects the inverter output performance [19]. Kanchan *et al.* [20] have achieved an effective for reducing the output common-mode voltage by considering the common-mode voltage factor as a weighting factor in the cost function. However, it is difficult to consider the determination of the weight coefficient. Therefore, this method is hard to accomplish in practical situations. Hoseini *et al.* [21], Wang *et al.* [22] proposed the concept of virtual vector that constructed by linear combination of basic vectors, by this way the entire control area of the inverter is fully utilized, and the utilization rate of the inverter control area is improved. Therefore, good inverter output performance and current tracking performance have been obtained at the same sampling frequency. However, because of adding the additional virtual vector, this method can greatly increase the calculation complexity as well as the switching frequency. What's more, adding the additional virtual vector makes it complex to obtain the triggering time of each switching device. The latter needs an external modulator or by using the look-up table, which is necessary for obtaining the trigger pulse signal of each switching device. Compared with the conventional MPC, the acquisition of the trigger pulse signal with adding the additional virtual vector becomes more complicated.

In this paper, voltage source inverter (VSI) under balance situation has been presented to study the VSI output common-mode voltage reduction method by using MPC. Moreover, a MPC method based on double vector optimized selection is proposed. This in turn benefit the reference tracking and

decreases the output current distortion rate by controlling the two non-zero voltage vectors in each sampling period. Similar to the conventional MPC method, the two voltage vectors obtained by the cost function optimization should make the errors between the reference values and real values smaller. Meanwhile, considering the problem of excessive switching frequency, the selection of the second vector should be optimized that the second voltage vector can be only selected from two voltage vectors adjacent to the first selected voltage vector. Therefore, the MPC via the double vector optimized selection method proposed in this paper can reduce the inverter output common-mode voltage due to discarding the zero vectors. At the same time, because of controlling the switch twice in one sampling period, the THD value is greatly reduced compared to the method of directly discarding the zero voltage vector. Meanwhile, compared to the adding virtual vector MPC method, which results in much higher switching frequency the method proposed in this paper, also increases the switching frequency but is much lower than the switching frequency of the adding virtual vector MPC method. In summary, the method proposed in this paper can effectively reduce the common-mode voltage and compensate for the reduction of the available voltage vector by controlling the switching action twice in one sampling period. Simultaneously, by limiting the selection range of the second voltage vector, the switching frequency as well as the switching loss is reduced.

The main contributions in this paper are concluded as follows: First, comparing with the conventional MPC method for three-phase two-level inverter, the proposed method in this paper can effectively reduce the output common-mode voltage of the inverter. Second, comparing with the zero-free vector MPC method, the problem of rising the THD due to the reduction of the available voltage vector is solved by controlling the switch action twice in one sampling period. Third, comparing with the adding virtual vector MPC method, which added virtual voltage vector to result in an excessive switching frequency and higher switching losses, the proposed method in this paper defines the selection range of the second voltage vector. Only two voltage vectors adjacent to the first voltage vector can be selected, so that the switching frequency is greatly reduced.

The remaining sections of this paper are organized as follows: Section II shows the analysis of common-mode voltage based on three-phase two-level inverter, Section III presents the conventional MPC methods for reducing common-mode voltage of two-level inverter, and Section IV shows the improved model prediction control for reducing the inverter output common-mode voltage proposed in this paper. Section V shows the simulation results among the conventional MPC methods for reducing common-mode voltage of two-level inverter and the proposed reduction method. Section VI presents the comparison experiment results among the conventional method, the zero-free vector method, the adding virtual vector method and proposed method.

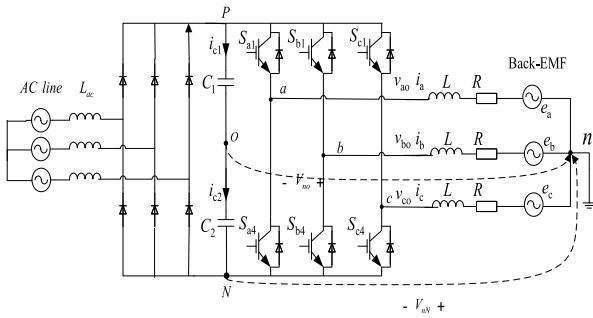


FIGURE 1. Main circuit topology of three-phase two-level inverter.

II. COMMON MODE-VOLTAGE ANALYSIS OF TWO-LEVEL INVERTER

Fig. 1 shows the main circuit topology of VSI with a three-phase two-level current structure. Each switch state can be defined as S_x ($x = 1, \dots, 6$) and the three legs switch state can be represented by S_a, S_b and S_c [26]. The three-phase two-level inverter has 8 switching states and can be defined as follows [26]:

$$\begin{cases} S_a = \begin{cases} 1 & \text{If } S_1 \text{ is turned on, } S_4 \text{ is turned off} \\ 0 & \text{If } S_4 \text{ is turned on, } S_1 \text{ is turned off} \end{cases} \\ S_b = \begin{cases} 1 & \text{If } S_2 \text{ is turned on, } S_5 \text{ is turned off} \\ 0 & \text{If } S_5 \text{ is turned on, } S_2 \text{ is turned off} \end{cases} \\ S_c = \begin{cases} 1 & \text{If } S_3 \text{ is turned on, } S_6 \text{ is turned off} \\ 0 & \text{If } S_6 \text{ is turned on, } S_3 \text{ is turned off} \end{cases} \end{cases} \quad (1)$$

Fig. 1 presents the inverter output common-mode voltage. In the three-phase two-level, VSI is considered as the potential difference between the load neutral point and the reference ground [24]. Since v_{oN} is much smaller than v_{no} , it is often ignored when calculating the output common-mode voltage. Hence, the inverter output common-mode voltage is the voltage between the neutral point of the inverter DC side and the three-phase star connection as follows [24]:

$$v_{CM} = v_{no} = \frac{(v_{ao} + v_{bo} + v_{co})}{3} \quad (2)$$

Combine equations (1) and (2), the relationship between the output common-mode voltage of the two-level three-phase inverter and the respective switching states can be obtained as follows [24]:

$$v_{CM} = \frac{V_{dc}}{3} \times (S_a + S_b + S_c) - \frac{V_{dc}}{2} \quad (3)$$

From equation (3), the amplitude of output common-mode voltage corresponding to each space voltage vector of inverter can be obtained as shown in Table 1.

It is obvious from Table 1 that the maximum value of the output common-mode voltage is $V_{dc}/2$. When utilizing the zero voltage vector (the switching state is all 0 or all 1), the value of the output common-mode voltage will reach the maximum value. According to this result, the most conventional control method for reducing the output common-mode

TABLE 1. The magnitude of common-mode voltage according to the switching states.

Voltage vector	Switch states	Common-mode voltage
V_0	(0,0,0)	$-V_{dc}/2$
V_1	(1,0,0)	$-V_{dc}/6$
V_2	(1,0,1)	$V_{dc}/6$
V_3	(0,1,0)	$-V_{dc}/6$
V_4	(0,1,1)	$V_{dc}/6$
V_5	(0,0,1)	$-V_{dc}/6$
V_6	(1,0,1)	$V_{dc}/6$
V_7	(1,1,1)	$V_{dc}/2$

voltage is to avoid using the zero voltage vector directly. That is, only the non-zero voltage vector of the output common-mode voltage is applied to synthesize the reference voltage vector for effectively reducing the output common-mode voltage.

III. CONVENTIONAL THREE-PHASE TWO-LEVEL PREDICTION COMMON-MODE VOLTAGE REDUCTION METHOD

Several literatures have proposed research methods to analyze and decrease the common-mode voltage. Among them, the zero-free vector MPC method is one of method to reduce the inverter output common-mode voltage. This method is able to effectively decrease the value of the inverter output common-mode voltage; however, discard of the available vector will disturb the tracking performance of the output current and cause large distortion of current output waveform. Another conventional method to reduce the inverter output common-mode voltage is considering the common-mode voltage reduction as a secondary control target. By establishing a cost function that considers the common-mode voltage factor, the output common-mode voltage is reduced. However, the additional common-mode voltage factor increases the cost function calculation and disturbs the output current tracking performance. According to the above method, literature [2] proposes a method for reducing the inverter output common-mode voltage by adding virtual vector. This method can provide better inverter output performance and current tracking performance under the same sampling frequency. While by this method control the switches action multiple times in one sampling period according to the voltage vector calculated by the cost function so the switching frequency is greatly increased. Therefore, the method of adding virtual vector can be only applied for low power inverter.

A. ZERO-FREE VECTOR MPC METHOD FOR REDUCING COMMON-MODE VOLTAGE

The conventional MPC method selects the optimal voltage vector by optimizing eight voltage vector include

six non-zero voltage vectors and two zero voltage vectors [4]. However, it can be seen from Table 1 that the zero voltage vector can cause higher inverter output common-mode voltage. In order to reduce the output common-mode voltage the author in literature [19] directly discarding the zero vector voltage vector in the optimization calculation to reduce the output common-mode voltage.

According to the space vector principle, the output voltage vector in the two-level inverter is obtained as follows [6]:

$$u_1 = \frac{2}{3}(u_{aN} + \alpha \times u_{bN} + \alpha^2 \times u_{cN}) \quad (4)$$

where α is the unit vector that represents the difference of each phase and equals to $e^{j2\pi/\beta}$.

The dynamic equation of the load current can be obtained by using Kirchhoff theorem as follows [6]:

$$v = Ri + L \frac{di}{dt} + e \quad (5)$$

The three-phase two-level inverter in the $\alpha\beta$ stationary coordinate system is determined as follows [25]:

$$\frac{d}{dt} \begin{bmatrix} i_{\alpha 1} \\ i_{\beta 1} \end{bmatrix} = -\frac{R_1}{L_1} \begin{bmatrix} i_{\alpha 1} \\ i_{\beta 1} \end{bmatrix} + \frac{1}{L_1} \begin{bmatrix} u_{\alpha 1} - e_{\alpha} \\ u_{\beta 1} - e_{\beta} \end{bmatrix} \quad (6)$$

Assuming the sampling period is T_s , and then the forward Euler approximation is substituted for the load current derivative, di/dt that approximately can be determined as follows [6]:

$$\frac{di}{dt} \approx \frac{i(k) - i(k-1)}{T_s} \quad (7)$$

The discretized output current average model can be obtained from equations (6) and (7) as follows:

$$\begin{bmatrix} i_{\alpha}(k) \\ i_{\beta}(k) \end{bmatrix} = \begin{bmatrix} i_{\alpha}(k-1) \\ i_{\beta}(k-1) \end{bmatrix} + \frac{T_s}{L} \begin{bmatrix} u_{\alpha}(k) \\ u_{\beta}(k) \end{bmatrix} - \begin{bmatrix} e_{\alpha}(k) \\ e_{\beta}(k) \end{bmatrix} \quad (8)$$

Due to comparing to the quick sampling frequency, the frequency of the back electromotive force vector (EMF) is much lower, so it can be assumed that $e(k+1) \approx e(k)$ [25]. The schematic diagram of model predictive control without delay compensation model is shown in Fig. 2. Considering the measurement of the load voltage and the load current, the back potential can be calculated as follows [5]:

$$e(k-1) = v(k-1) - \frac{L}{T_s}i(k) - (R - \frac{L}{T_s})i(k-1) \quad (9)$$

As shown in Fig. 2 there is a certain delay in practical controllers, which leads to inaccurate control. The need for the controller to perform prediction calculations causes the time delay τ . In the ideal case, when $t = t_{k+1}$, the controlled should reach position ① in Fig. 2. However, due to the delay time, the inverter still uses the switch state of the previous moment during $[t_k, t_k + \tau]$ period. As a result, when $t = t_k$, the controlled cannot reach position ①, it can only reach position ② in Fig. 2, which result in a large mistake between the reference value and the real value.

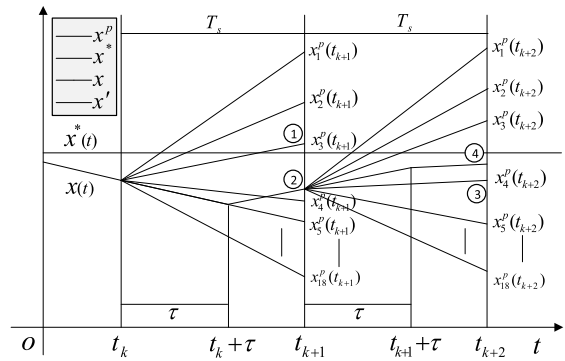


FIGURE 2. Schematic diagram of predictive control without delay compensation model.

The MPC control proposed in this paper considers the time delay of one period, which can be expressed as follows [6]:

$$\begin{bmatrix} i_{\alpha}(k+1) \\ i_{\beta}(k+1) \end{bmatrix} = \begin{bmatrix} i_{\alpha}(k) \\ i_{\beta}(k) \end{bmatrix} + \frac{T_s}{L} \begin{bmatrix} u_{\alpha}(k+1) \\ u_{\beta}(k+1) \end{bmatrix} - \begin{bmatrix} e_{\alpha}(k+1) \\ e_{\beta}(k+1) \end{bmatrix} \quad (10)$$

The conventional finite set model predictive control uses a predefined cost function. The cost function is set in order to make the real current as close as the reference current, which can be defined as follow [2]:

$$g = |i_{\alpha}^*(k+1) - i_{\alpha}(k+1)| + |i_{\beta}^*(k+1) - i_{\beta}(k+1)| \quad (11)$$

Considering that the zero voltage vector will generate a higher output common-mode voltage, the literature [18] discards the zero voltage vector directly when using MPC so that the output common-mode voltage can be reduced from $1/2V_{dc}$ to $1/6V_{dc}$.

In the zero-free vector MPC method, it is just needed to predict the load current and find the optimal result of the cost function using the six switching states. Moreover, there are no major changes between the improved method and the conventional predictive control method. However, this method depends on discarding the zero vector directly to reduce the common-mode voltage. Moreover, due to the reduction of the available vectors, the tracking performance of the output current, and the inverter output performance is affected.

B. MPC STRATEGY BASED ON VIRTUAL VOLTAGE VECTOR SELECTION TO REDUCE COMMON MODE VOLTAGE

The zero-free vector MPC method although capable of reducing the output common-mode voltage amplitude from $1/2V_{dc}$ to $1/6V_{dc}$, it causes a large current distortion. In order to solve the above problems, literatures [20]–[22] proposed a MPC common-mode voltage reduction method based on adding virtual voltage vector.

In [20], 12 virtual vectors are constructed by a linear combination of six non-zero basic voltage vectors. The MPC method based on virtual voltage vector selection can reduce

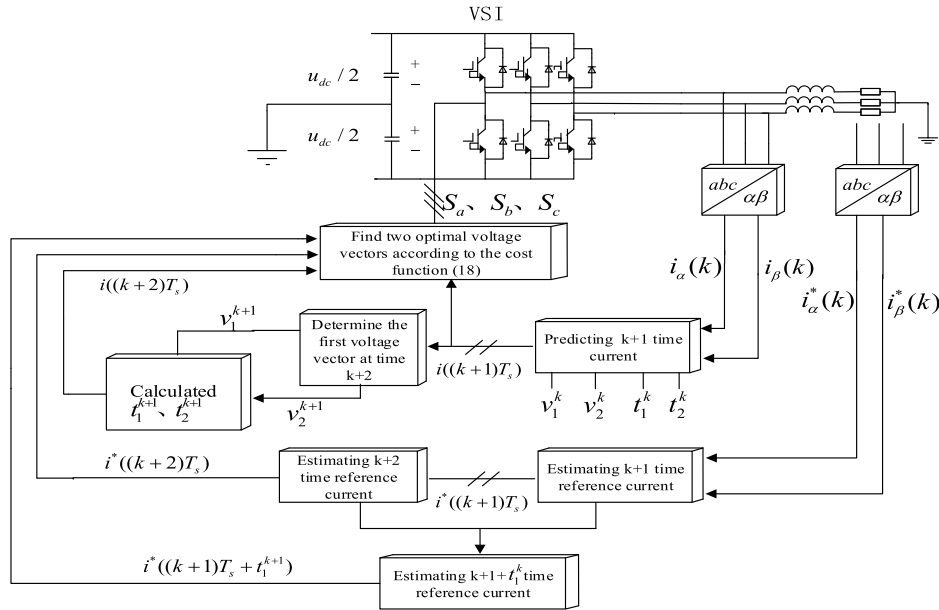


FIGURE 3. The proposed model predictive control block diagram.

the amplitude of the inverter output common-mode voltage and improve current tracking performance. However, the calculation process, the load current prediction and the corresponding cost function calculations need to be repeated 18 times. While the conventional MPC only needs to be repeated 7 times. Compared with the conventional MPC, adding the virtual vector MPC method will increase the calculation complexity. When adding the virtual vector, it needs to compare the external modulator with the carrier to obtain the trigger pulse signal of each leg-switching device. Furthermore, the acquisition of the pulse signal after adding the virtual vector is complicated.

IV. IMPROVED MODEL PREDICTION CONTROL FOR COMMON-MODE VOLTAGE REDUCTION

As described in Section III, although the method of zero-free vector MPC method can reduce the common-mode voltage from $1/2V_{dc}$ to $1/6V_{dc}$, it will cause greater current distortion. Moreover, the method of adding virtual vector will increase the amount of calculation during the process and it is more complicated to acquire the pulse signal. What's more, the method of adding virtual vector causes high switching frequency and high switching losses. In order to solve these problems, this paper proposes a MPC method based on double vector optimized selection for reducing the inverter output common-mode voltage. The flowchart of the overall system structure is presented in Fig. 3.

A. MODEL PREDICTIVE CONTROL METHOD VIA DOUBLE VECTOR

In contrast to the conventional MPC method and the adding virtual vector MPC method, that only one voltage vector can

be selected from the finite voltage vector in each sampling period. This paper proposes a MPC method based on double vector for the three-phase two-level inverter. In the zero-free vector MPC method, the output steady-state performance is unsatisfactory because of the limit of the number of transformer voltage vectors. For improving the steady-state performance of the MPC and reduce the computational complexity of the control method; the proposed control method can optimize two voltage vectors in each sampling period. The control method in advance uses the conventional MPC method to select the first non-zero vector according to the cost function in equation (11). Then, after selecting the first voltage vector, the second vector can only select the two vectors adjacent to the first voltage vector so the switching frequency can be greatly reduced. Therefore, the relation between the two vector active time and the sampling time can be defined as:

$$t_1^k + t_2^k = T_s \quad (12)$$

where, the action time of the first voltage vector and the second voltage vector at the k th time can be defined as t_1, t_2 respectively. The action time of the two voltage vectors must be greater than zero, and smaller than the sampling period. The predicted current based on the double vector optimized selection can be obtained as follows:

$$i((k+1)T_s) = i(kT_s) + \frac{t_1^k}{L} [v_1^k - Ri(kT_s) - e(kT_s)] + \frac{t_2^k}{L} [v_2^k - Ri(kT_s + t_1^k) - e(kT_s + t_1^k)] \quad (13)$$

According to equation (9), the back electromotive force under the predictive control of the double vector model can

be obtained as follows:

$$\begin{aligned}
 e(kT_s) &\approx e((k-1)T_s) = \frac{t_1^{k-1}}{T_s} [v_1^{k-1} - Ri((k-1)T_s)] \\
 &+ \frac{t_2^{k-1}}{T_s} [v_2^{k-1} - Ri((k-1)T_s) + t_1^{k-1}] \\
 &- \frac{L}{T_s} [i(kT_s) - i((k-1)T_s)]
 \end{aligned} \tag{14}$$

B. CALCULATION OF VOLTAGE VECTOR ACTION TIME

After the determination of v_1^{k+1} and v_2^{k+1} , the action times t_1^{k+1} and t_2^{k+1} should be considered. The selection principle of t_1^{k+1} and t_2^{k+1} is to making the prediction current as close as to the reference current. Therefore, the calculations of the action times of two-voltage vector are obtained by considering the follows:

$$\frac{\partial g}{\partial t_1^{k+1}} = 0 \tag{15}$$

Then the action times of the two voltage vectors can be obtained as follows:

$$\begin{aligned}
 t_1^{k+1} &= \frac{V_{\Delta\alpha}[Le_{2\alpha} + T_s(V_{\Delta\alpha} - V_{H\alpha})] + V_{\Delta\beta}[Le_{2\beta} + T_s(V_{\Delta\beta} - V_{H\beta})]}{(V_{\Delta\alpha})^2 + (V_{\Delta\beta})^2}
 \end{aligned} \tag{16}$$

$$\begin{aligned}
 t_2^{k+1} &= T_s - t_1^{k+1}
 \end{aligned} \tag{17}$$

where,

$$V_{\Delta n} = v_{1n}^{k+1} - v_{2n}^{k+1} \tag{18}$$

$$V_{Hn} = v_{1n}^{k+1} - Ri_n((k+1)T_s) - e_n(kT_s) \tag{19}$$

$$e_{2n} = i_n^*((k+2)T_s) - i_n((k+1)T_s) \tag{20}$$

where n can be α or β .

C. VOLTAGE VECTOR OPTIMIZATION

The schematic diagram of MPC method based on double vector is shown in Fig. 4. As shown in Fig. 4, in the conventional MPC method based on the double vector, the two non-zero voltage vectors need work simultaneously in each sampling period for reducing the common-mode voltage and the total harmonic distortion (THD) rate. However, through this method, the calculation is complexity and the switching frequency is high [16]. From this, a MPC method based on double vector optimized selection has been proposed in this paper.

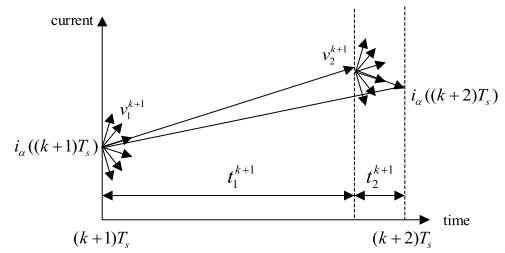


FIGURE 4. Schematic diagram of model predictive control method based on double vector.

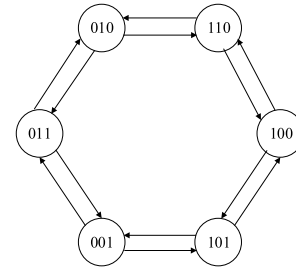


FIGURE 5. Optimized voltage vector selection method.

Fig. 5 shows the voltage vector optimized selection method. In contrast with the conventional MPC method based on the double vector, the proposed method selects the first optimal vector in advance according to the conventional model predictive control method. Then select the second voltage vector based on the first vector that the second voltage vector can be only selected adjacent to the first voltage vector for reducing the calculation, the switching frequency and the common-mode voltage.

According to Fig. 5, after the first vector is selected, the second vector can be only selected from adjacent first nonzero voltage vector. The amount of calculation can be greatly reduced by using this vector performs optimization operations. At the same time, the reference current and load current after applying the first voltage vector need to be considered and the cost function is modified to equation (21), as shown at the bottom of this page. The action time of the first vector is modified to equation (22), as shown at the bottom of this page. In practice controls, because of the blanking time and dead time of the switching device [31], it is also necessary to avoid the three legs active at the same time. The method proposed in this paper is completely avoid the working state of the inverter two-leg and three-leg simultaneous action for reducing the switching frequency. At the same time, the output common-mode voltage can be effectively reduced without applying

$$\begin{aligned}
 g &= |i_{\alpha}^*((k+2)T_s) - i_{\alpha}((k+2)T_s)| + |i_{\beta}^*((k+2)T_s) - i_{\beta}((k+2)T_s)| + |i_{\alpha}^*((k+1)T_s + t_1^{k+1}) - i_{\alpha}((k+1)T_s + t_1^{k+1})| \\
 &+ |i_{\beta}^*((k+1)T_s + t_1^{k+1}) - i_{\beta}((k+1)T_s + t_1^{k+1})|
 \end{aligned} \tag{21}$$

$$t_1^{k+1} = \frac{V_{\Delta\alpha}[Le_{2\alpha} + T_s(V_{\Delta\alpha} - V_{H\alpha})] + V_{\Delta\beta}[Le_{2\beta} + T_s(V_{\Delta\beta} - V_{H\beta})] - L[e_{1\alpha}(\frac{L}{T_s}i_{d\alpha}^* - V_{H\alpha}) + e_{1\beta}(\frac{L}{T_s}i_{d\beta}^* - V_{H\beta})]}{(V_{\Delta\alpha})^2 + (V_{\Delta\beta})^2 + (\frac{L}{T_s}i_{d\alpha}^* - V_{H\alpha})^2 + (\frac{L}{T_s}i_{d\beta}^* - V_{H\beta})^2} \tag{22}$$

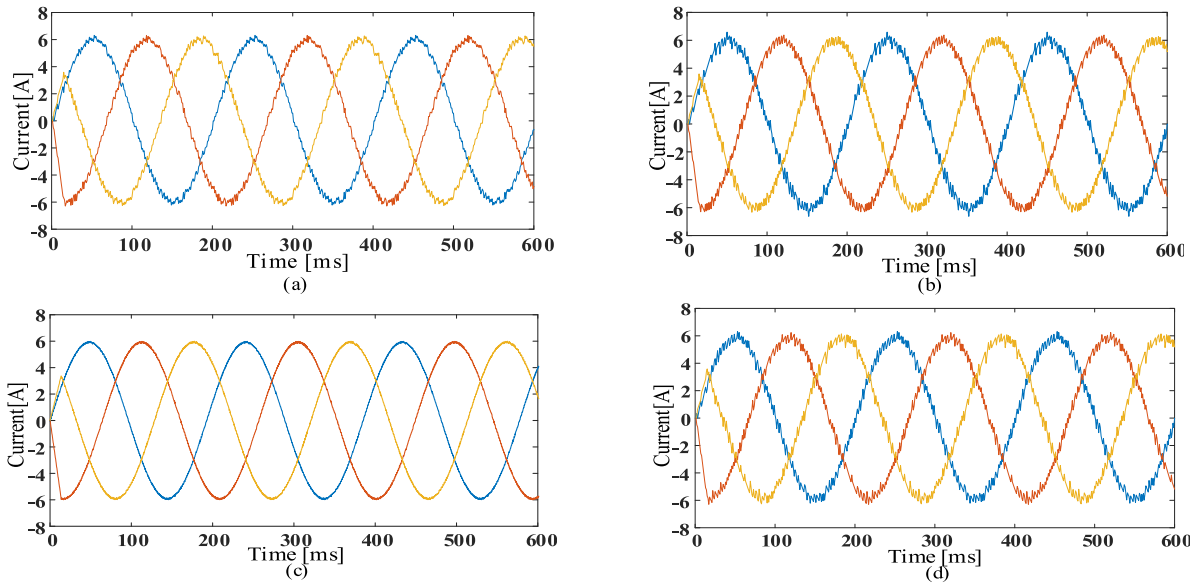


FIGURE 6. Simulated waveforms: (a) conventional MPC method (b) zero-free vector MPC method, (c) adding virtual vector MPC method (d) proposed method.

zero voltage vector, where, $e_{1n} = i_n^*((k+1)T_s) - i_n((k+1)T_s)$, $i_{dn}^* = i_n^*((k+2)T_s) - i_n^*((k+1)T_s)$.

V. SIMULATION ANALYSIS AND DISCUSSION

The simulation analysis is carried out in MATLAB/Simulink in order to verify the effect of the proposed MPC method for the inverter output common-mode voltage reduction. The inverter operates at rated power with unity power factor. The simulation time is set to 0.15s, and the simulation parameters are shown in Table 2.

TABLE 2. The simulation parameters.

Parameter	Value
DC side voltage V_{dc}	100V
Resistance	2.5Ω
Inductance	30e-3H
Sampling frequency	10kHz
Reference current amplitude	6A
Reference frequency	100πHz
DC side capacitor C_1, C_2	4400μF

Fig. 6 shows the simulated output current waveforms using conventional MPC method, the zero-free vector MPC method, adding virtual voltage vector MPC method and the proposed method in this paper respectively. It is obvious from the figure that using the zero-free vector MPC method disturbs the current tracking performance of the output current. In contrast, the virtual vector method can achieve better current quality due to the addition of virtual vectors. Compare to all the four methods, the proposed method in this paper can improve the tracking performance of current compare with the zero-free vector MPC method.

Fig. 7(a) shows a simulation waveforms of the output phase voltage and the common-mode voltage when using the conventional MPC method. It can be seen from the figure that because of the existence of zero vector, the inverter output common-mode voltage can be achieved $V_{dc}/2$. The latter not only causes additional power losses of the motor, but also affects the reliability of the motor operation. At the same time, it will threaten the safe and stable operation of the grid. Fig. 7(b) shows the inverter output current spectrum using the conventional MPC method. It can be seen from the figure that the THD value of the output current can be controlled to a lower range using the conventional MPC method.

Fig. 8 (a) shows the output phase voltage and common-mode voltage waveforms of the inverter when using zero-free vector MPC method. As shown in Fig. 8, when the zero voltage vector is discarded, the common-mode voltage is reduced from $V_{dc}/2$ to $V_{dc}/6$. However, it can be seen that the current tracking performance is worse because of discarding the zero vector and it will increase the current distortion rate as well as the THD value.

Fig. 9 (a) shows the output phase voltage and common-mode voltage waveform of the inverter when adding virtual voltage vector. Fig. 9 (b) shows the inverter output current spectrum when adding additional virtual. It can be seen from the figure that by adding additional virtual voltage vector, the output common-mode voltage amplitude is reduced and the value of THD became lower. However, since the virtual vector is synthesized by two base vectors, the switching frequency is greatly increased, which complicates the control algorithm.

Fig. 10 (a) shows the output common-mode voltage waveform of the common-mode voltage reduction method based on the double vector optimized selection proposed in this

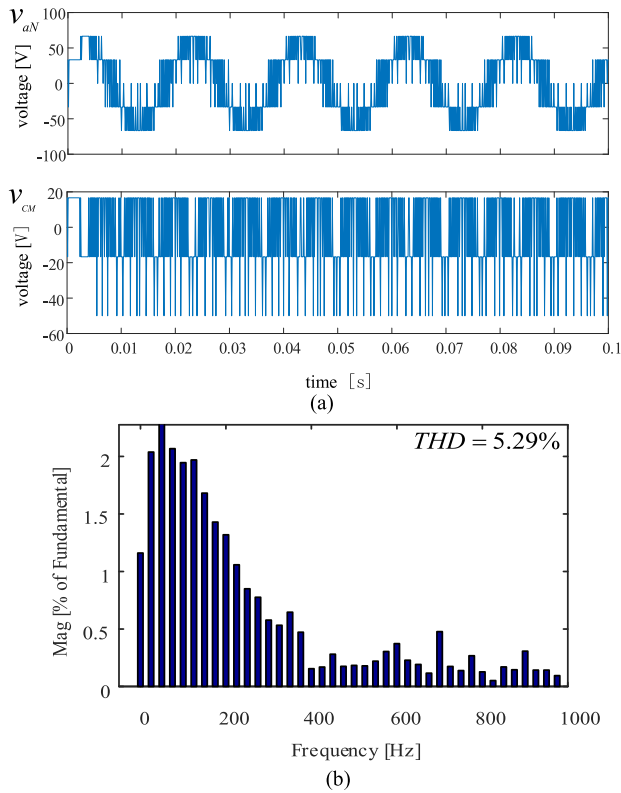


FIGURE 7. (a) Inverter output phase voltage and common mode voltage waveform using conventional model predicts control (b) Inverter output current spectrum diagram of conventional model predictive control.

paper. It can be seen from this figure that the proposed method can reduce the common-mode voltage effectively. At the same time, it can be seen from Fig. 10 (b) that the method proposed in this paper controls two voltage vectors during each sampling period, so that the current tracking performance is further improved and the current harmonic distortion rate is further reduced.

VI. EXPERIMENTAL VERIFICATION

For further verify the effectiveness of the proposed control method, an experiment constructs a control platform based on Simulink-Real-Time system is introduced. Fig. 11 shows the structure diagram of the experimental system. The system uses a host and Simulink-Real-Time system as part of the controller for performs processing. Therefore, it can avoid the complicated programming processes such as the digital signal processing application. The rectifier circuit in this paper uses a three-phase uncontrolled rectifier bridge to rectify the AC voltage into DC voltage. Furthermore, by adjusting the three-phase voltage regulator, the DC side voltage after three-phase rectification through the three-phase uncontrolled rectifier bridge can reaches 100V. Table 3 presents the main parameters of the experiment system.

It is obvious from the experimental result that the experimental results are the same as the simulation results using the four methods are similar. Compare with

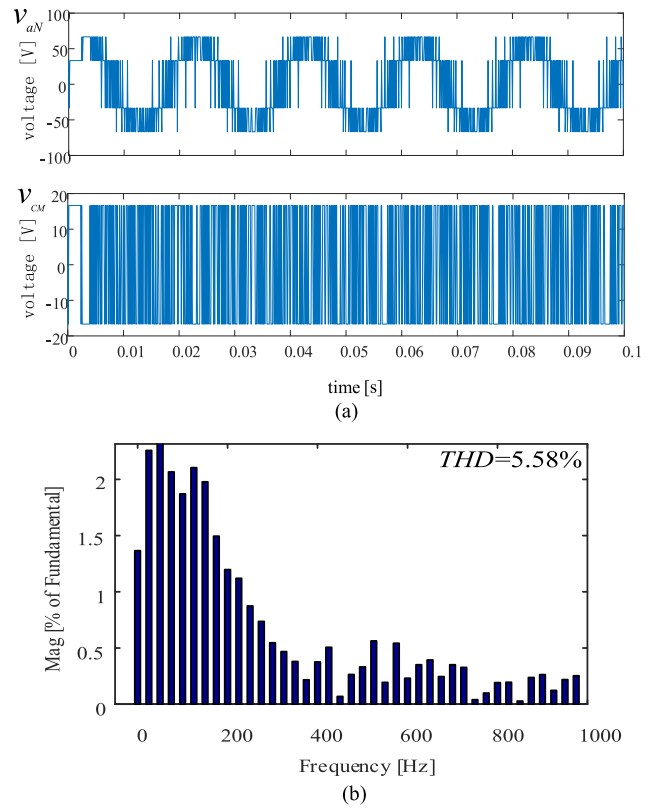


FIGURE 8. (a) Inverter output phase voltage and common mode voltage waveform using zero-free vector MPC method (b) Inverter output current spectrum when discarding zero vector MPC method.

TABLE 3. Main parameters of the experiment.

Parameter	Value
DC side voltage V_{dc}	100V
DC side capacitor C_1, C_2	4400 μ F
Inductance/resistance	25mH/2.5 Ω
Maximum allowable peak current I_{max}	6A
Sampling frequency T_s	10 kHz

Fig. 12 (a), 13 (a), 14 (a) and 15 (a), it can be seen that both the adding virtual voltage vector MPC method and proposed method can benefit the reference tracking performance of the current. Furthermore, because of using only V_0 and without using V_7 in the control algorithm, the value of common-mode voltage for the conventional MPC method is between $V_{dc}/6$ and $V_{dc}/2$ as shown in Fig. 12 (b). As shown in Fig. 13 (b), 14 (b) and 15 (b), the output common-mode voltage are reduced at the range of $-V_{dc}/6$ to $V_{dc}/6$ depending on discarding the zero vectors. However, due to adding additional virtual voltage vector, the switching frequency in Fig. 14 (b) became very high.

The comparison result of the proposed method with the conventional method, the zero-free vector MPC method, the adding virtual vector MPC method in frequency spectrum of the load currents are shown in

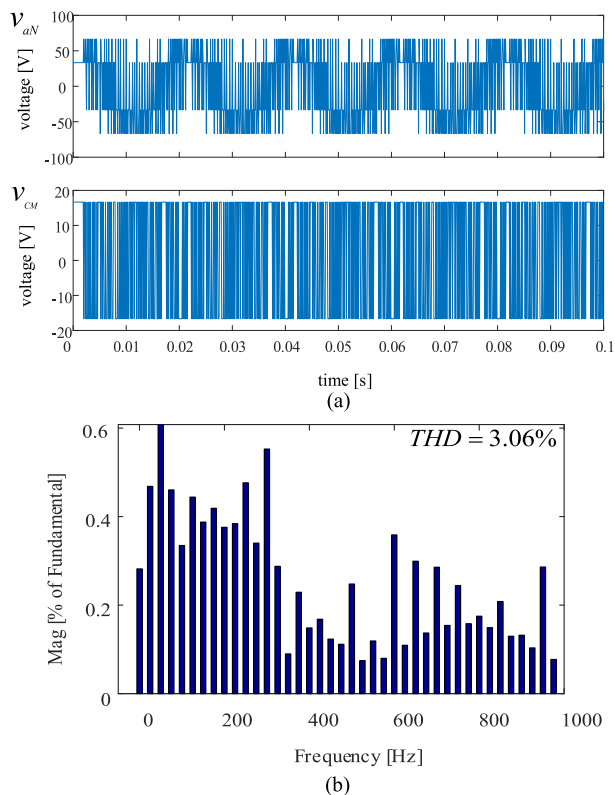


FIGURE 9. (a) Inverter output phase voltage and common mode voltage waveform of adding virtual vector MPC method (b) Inverter output current spectrum when adding voltage vector MPC method.

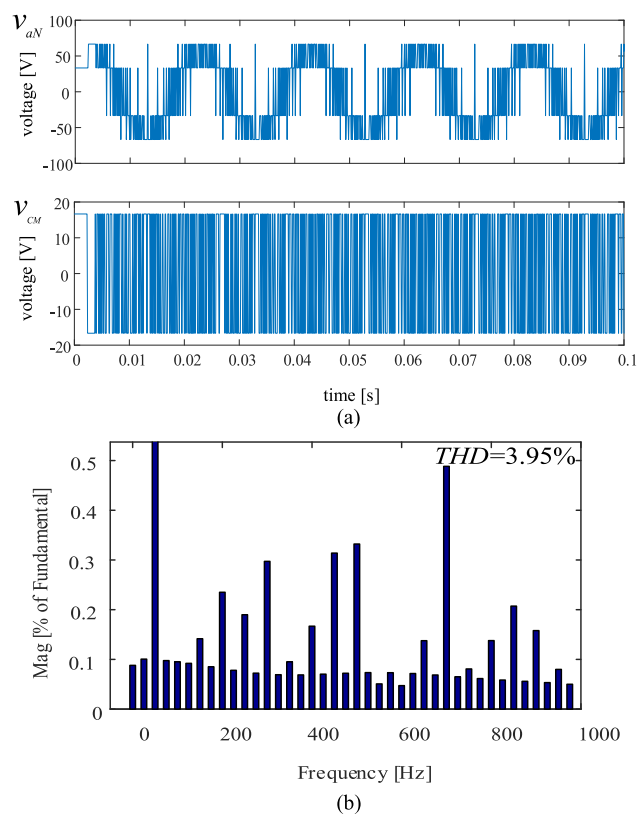


FIGURE 10. (a) Inverter output phase voltage and common-mode voltage waveform using proposed method (b) Inverter output current spectrum diagram of the proposed method.

Figs. 12 (c), 13 (c), 14 (c) and 15(c). In addition, although the proposed method in this paper has a higher THD compared with MPC based on virtual voltage vector it presents that compare to the conventional method and the zero-free vector MPC method, the proposed method can efficiently reduce the THD value.

Furthermore, it can be seen from the comparison result among the four methods that the proposed method can effectively reduce the inverter output common-mode voltage. At the same time, compared with the conventional method of reducing common-mode voltage, the proposed method can reduce the current harmonic distortion rate as well as improving the output current performance.

Fig.16 shows the switching frequency comparison results of the proposed method with the conventional MPC method, zero-free vector MPC method and adding virtual vector MPC method. As shown in Fig. 16, the zero-free vector MPC method has the lowest switching frequency due to discarding of zero voltage vector. In contrast, the adding virtual vector MPC method greatly increases the switching frequency due to the addition of the virtual voltage vector. Although the proposed method has a higher switching frequency than zero-free vector MPC method, its switching frequency is much lower than the method of adding virtual voltage vector.

Table 4 presents the comparison results among the propose method and the conventional methods, the zero-free

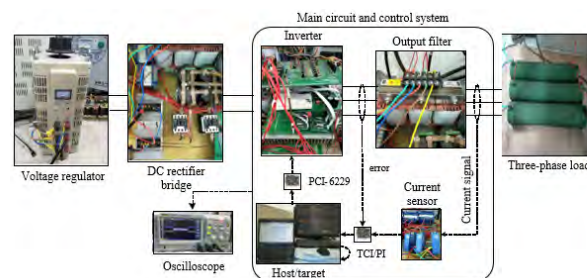


FIGURE 11. Structure diagram of experiment system.

vector MPC method and adding virtual vector MPC method. According to Table 4, the proposed method can effectively reduce the output common-mode voltage of the inverter at the same range as the zero-free vector MPC method and the adding virtual vector MPC method. Simultaneously, the THD value is greatly reduced compared to the zero-free vector MPC method. Comparing to the method that adding virtual vector results in a much higher switching frequency the proposed method also increases the switching frequency but is much lower than the switching frequency of the adding virtual vector method. Although the THD value of the proposed method is slightly higher than adding the virtual vector MPC method, but is much lower than the conventional MPC method and the zero-free vector MPC method.

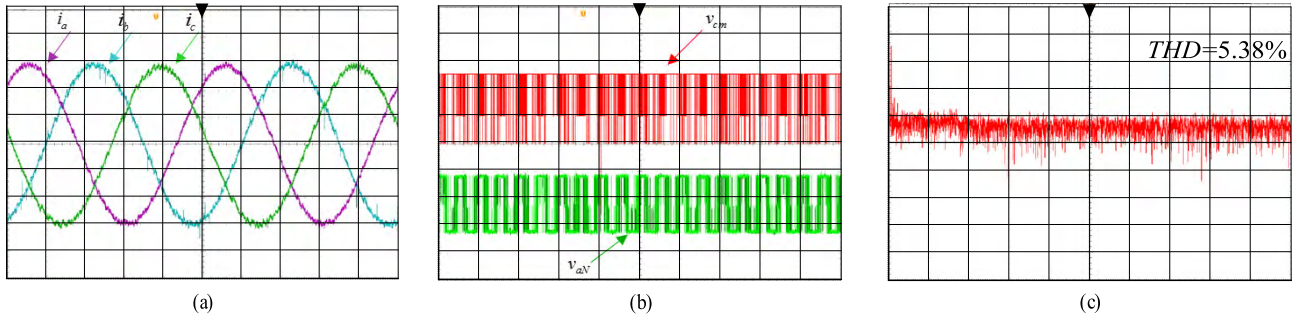


FIGURE 12. Experimental waveforms of the conventional MPC method with $T_s = 100\mu s$: (a) the three phase load currents (0.4A/div and 4ms/div), (b) phase voltage (7.7V/div and 4ms/div) and common-mode voltage (7.7V/div and 4ms/div), and (c) frequency spectrum of the a-phase load current (10mA/div and 1.25kHz/div).

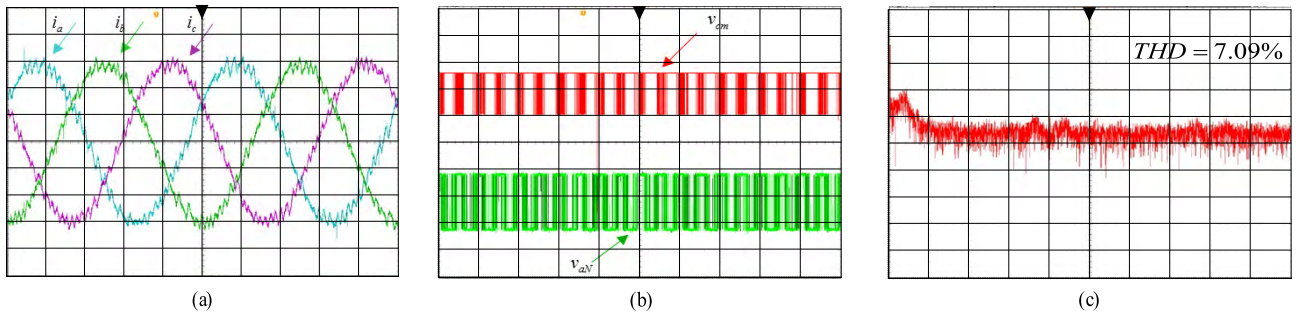


FIGURE 13. Experimental waveforms of the zero-free vector MPC method with $T_s = 100\mu s$: (a) the three phase load currents (0.4A/div and 4ms/div), (b) phase voltage (7.7V/div and 4ms/div) and common-mode voltage (7.7V/div and 4ms/div), and (c) frequency spectrum of the a-phase load current (10mA/div and 1.25kHz/div).

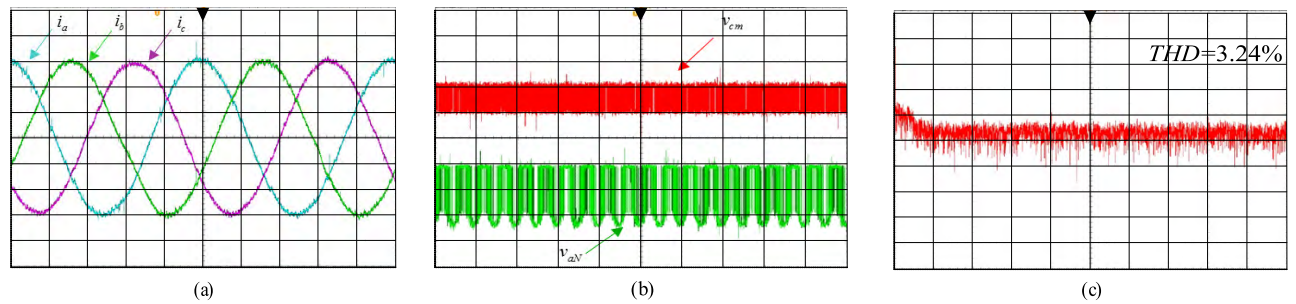


FIGURE 14. Experimental waveforms of the adding virtual vector MPC method with $T_s = 100\mu s$: (a) the three phase load currents (0.4A/div and 4ms/div), (b) phase voltage (7.7V/div and 4ms/div) and common-mode voltage (7.7V/div and 4ms/div), and (c) frequency spectrum of the a-phase load current (10mA/div and 1.25kHz/div).

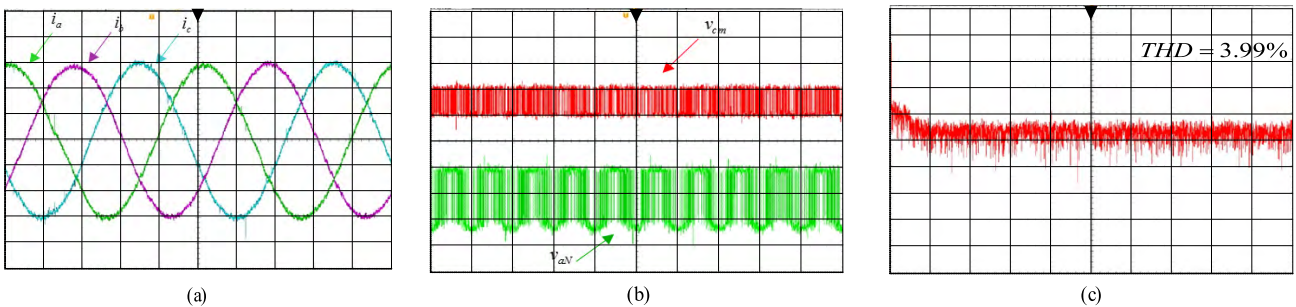


FIGURE 15. Experimental waveforms of proposed method in this paper with $T_s = 100\mu s$: (a) the three phase load currents (0.4A/div and 4ms/div), (b) phase voltage (7.7V/div and 4ms/div) and common-mode voltage (7.7V/div and 4ms/div), and (c) frequency spectrum of the a-phase load current (10mA/div and 1.25kHz/div).

Fig. 17 shows the output current waveform and the output common-mode voltage waveform. When the inverter is operating at the proposed method with a reference load current

stepping up from 5A to 7A at 50ms and then stepping down from 7A to 5A at 70ms. As shown in Fig. 17, the load current well tracks the reference current with low distortions.

TABLE 4. Comparison results of the proposed method with the conventional method, zero-free vector method and adding virtual vector method.

Method	Common-mode voltage amplitude /V		THD		Switching frequency/Hz	
	simulation	experiment	simulation	experiment	simulation	experiment
Conventional MPC method	50	50	5.29%	5.38%	4700	4960
Zero-free vector MPC method	16.67	16.67	5.58%	7.09%	4333	4580
Adding virtual vector method	16.67	16.67	3.06%	3.24%	6233.3	6956
Proposed method	16.67	16.67	3.95%	3.99%	5023	5241

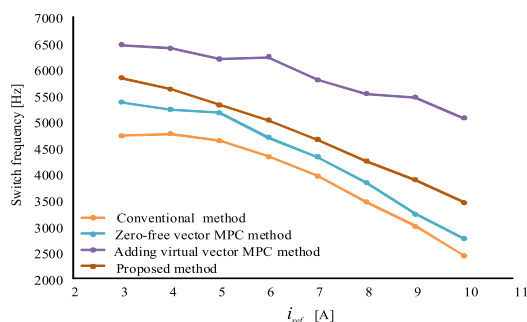


FIGURE 16. Comparison results between the proposed method and the conventional method, zero-free vector MPC method and adding virtual vector MPC method in switching frequency.

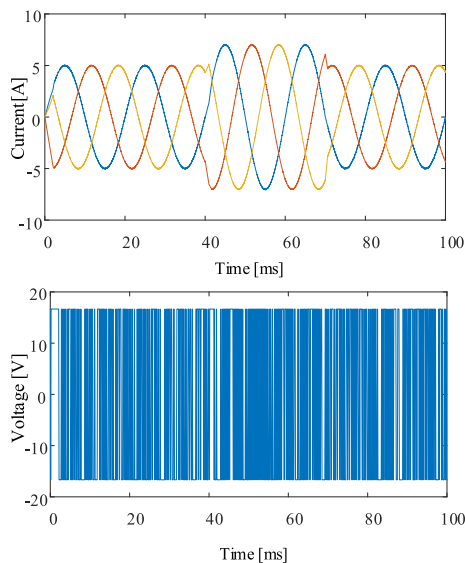


FIGURE 17. Current waveform and output common-mode voltage waveform in dynamic situations.

Simultaneously, it can be seen from the output common-mode voltage waveform diagram that the proposed method can also effectively reduce the common-mode voltage of the inverter in the same range even when the output current of the inverter is changed in 50ms and 70ms.

VII. CONCLUSION

In order to reduce the effect of the high output common-mode voltage in the control of three-phase two-level inverter,

a model predictive control via double vector optimized selection is proposed in this paper. In the context of the conventional MPC method, zero-free vector MPC and the adding virtual vector MPC method, this paper proposes a model predictive control method that controls two vectors in one sampling period to achieve effective reduction of the inverter output common-mode voltage. The simulation analysis and the experimental results show that the proposed method can effectively reduce the inverter output common-mode voltage. Moreover, comparing to the zero-free vector MPC method, the proposed method can improve the tracking performance of the output current and reduce the harmonic distortion rate of the output current. Simultaneously, according to the method of adding virtual vector results in high switching frequency and large switching losses, the proposed method limiting the selection range of the second voltage vector, so the switching frequency as well as the switching losses can be greatly reduced. Finally, how to reduce the occurrence of excessive common-mode voltage due to the existence of the blanking time under actual conditions as well as how to control the inverter under the unbalance situation will be the next important problem to be analyzed and solved.

REFERENCES

- [1] Q. Chen, X. Luo, L. Zhang, and S. Quan, "Model predictive control for three-phase four-leg grid-tied inverters," *IEEE Access*, vol. 5, pp. 2834–2841, 2017.
- [2] Y. Yang, H. Wen, and D. Li, "A fast and fixed switching frequency model predictive control with delay compensation for three-phase inverters," *IEEE Access*, vol. 5, pp. 17904–17913, 2017.
- [3] S. Rojas and A. Gensior, "Instantaneous average prediction of the currents in a PWM-controlled two-level converter," *IEEE Trans. Ind. Electron.*, vol. 66, no. 1, pp. 397–406, Jan. 2019.
- [4] A. M. Hava and E. Ün, "A high-performance PWM algorithm for common-mode voltage reduction in three-phase voltage source inverters," *IEEE Trans. Power Electron.*, vol. 26, no. 7, pp. 1998–2008, Jul. 2011.
- [5] E. A. Kumar, K. C. Sekhar, and R. S. Rao, "Model predictive current control of a three-phase T-type NPC inverter to reduce common mode voltage," *J. Circuits, Syst. Comput.*, vol. 27, no. 2, 2017, Art. no. 1850028.
- [6] H.-C. Moon, J.-S. Lee, and K.-B. Lee, "A robust deadbeat finite set model predictive current control based on discrete space vector modulation for a grid-connected voltage source inverter," *IEEE Trans. Energy Convers.*, vol. 33, no. 4, pp. 1719–1728, Dec. 2018.
- [7] H.-N. Nguyen and H.-H. Lee, "A modulation scheme for matrix converters with perfect zero common-mode voltage," *IEEE Trans. Power Electron.*, vol. 31, no. 8, pp. 5411–5422, Aug. 2016.
- [8] R. M. Tallam, R. J. Kerkman, D. Leggate, and R. A. Lukaszewski, "Common-mode voltage reduction PWM algorithm for AC drives," *IEEE Trans. Ind. Appl.*, vol. 46, no. 5, pp. 1959–1969, Sep. 2010.

- [9] M. M. Renge and H. M. Suryawanshi, "Three-dimensional space-vector modulation to reduce common-mode voltage for multilevel inverter," *IEEE Trans. Ind. Electron.*, vol. 57, no. 7, pp. 2324–2331, Jul. 2010.
- [10] H. Akagi and S. Tamura, "A Passive EMI filter for eliminating both bearing current and ground leakage current from an inverter-driven motor," *IEEE Trans. Power Electron.*, vol. 21, no. 5, pp. 1459–1469, Sep. 2006.
- [11] C. Qin, C. Zhang, A. Chen, X. Xing, and G. Zhang, "A space vector modulation scheme of the quasi-Z-source three-level T-type inverter for common-mode voltage reduction," *IEEE Trans. Ind. Electron.*, vol. 65, no. 10, pp. 8340–8350, Oct. 2018.
- [12] A. Edpuganti and A. K. Rathore, "Optimal pulsewidth modulation for common-mode voltage elimination scheme of medium-voltage modular multilevel converter-fed open-end stator winding induction motor drives," *IEEE Trans. Ind. Electron.*, vol. 64, no. 1, pp. 848–856, Jan. 2017.
- [13] Q.-H. Tran and H.-H. Lee, "An advanced modulation strategy for three-to-five-phase indirect matrix converters to reduce common-mode voltage with enhanced output performance," *IEEE Trans. Ind. Electron.*, vol. 65, no. 7, pp. 5282–5291, Jul. 2018.
- [14] T.-K. T. Nguyen and N.-Van Nguyen, "An efficient four-state zero common-mode voltage PWM scheme with reduced current distortion for a three-level inverter," *IEEE Trans. Ind. Electron.*, vol. 65, no. 2, pp. 1021–1030, Feb. 2018.
- [15] G. Yan, D. Liu, J. Li, and G. Mu, "A cost accounting method of the Li-ion battery energy storage system for frequency regulation considering the effect of life degradation," *Protection Control Mod. Power Syst.*, vol. 3, no. 3, pp. 43–51, 2018.
- [16] L. Wang, H. Dan, Y. Zhao, Q. Zhu, T. Peng, Y. Sun, and P. Wheeler, "A finite control set model predictive control method for matrix converter with zero common-mode voltage," *IEEE J. Emerg. Sel. Topics Power Electron.*, vol. 6, no. 1, pp. 327–338, Mar. 2018.
- [17] Y.-S. Kim and S.-K. Sul, "A novel ride-through system for adjustable-speed drives using common-mode voltage," *IEEE Trans. Ind. Appl.*, vol. 37, no. 5, pp. 1373–1382, Sep. 2001.
- [18] Y. Zhang and H. Yang, "Generalized two-vector-based model-predictive torque control of induction motor drives," *IEEE Trans. Power Electron.*, vol. 30, no. 7, pp. 3818–3829, Jul. 2015.
- [19] G. Mondal, K. Gopakumar, P. N. Tekwani, and E. Levi, "A reduced-switch-count five-level inverter with common-mode voltage elimination for an open-end winding induction motor drive," *IEEE Trans. Ind. Electron.*, vol. 54, no. 4, pp. 2344–2351, Aug. 2007.
- [20] R. S. Kanchan, P. N. Tekwani, and K. Gopakumar, "Three-level inverter scheme with common mode voltage elimination and DC link capacitor voltage balancing for an open-end winding induction motor drive," *IEEE Trans. Power Electron.*, vol. 21, no. 6, pp. 1676–1683, Nov. 2006.
- [21] S. K. Hoseini, J. Adabi, and A. Sheikholeslami, "Predictive modulation schemes to reduce common-mode voltage in three-phase inverters-fed AC drive systems," *IET Power Electron.*, vol. 7, no. 4, pp. 840–849, Apr. 2014.
- [22] X. Wang, J. Zou, L. Ma, J. Zhao, C. Xie, K. Li, L. Meng, and J. M. Guerrero, "Model predictive control methods of leakage current elimination for a three-level T-type transformerless PV inverter," *IET Power Electron.*, vol. 11, no. 8, pp. 1492–1498, Jul. 2018.
- [23] G. Li, G. Li, and M. Zhou, "Model and application of renewable energy accommodation capacity calculation considering utilization level of inter-provincial tie-line," *Protection Control Mod. Power Syst.*, vol. 4, no. 4, pp. 1–12, 2019.
- [24] S. Almér, S. Mariéthoz, and M. Morari, "Sampled data model predictive control of a voltage source inverter for reduced harmonic distortion," *IEEE Trans. Control Syst. Technol.*, vol. 21, no. 5, pp. 1907–1915, Sep. 2013.
- [25] S. Kwak and S. Mun, "Common-mode voltage mitigation with a predictive control method considering dead time effects of three-phase voltage source inverters," *IET Power Electron.*, vol. 8, no. 9, pp. 1690–1700, Sep. 2015.
- [26] T. D. Nguyen and H.-H. Lee, "Modulation strategies to reduce common-mode voltage for indirect matrix converters," *IEEE Trans. Ind. Electron.*, vol. 59, no. 1, pp. 129–140, Jan. 2012.
- [27] H.-C. Moon, J.-S. Lee, J.-H. Lee, and K.-B. Lee, "Model predictive control of a grid-connected inverter to reduce current ripples and computation loads," in *Proc. IEEE Appl. Power Electron. Conf. Exposit. (APEC)*, Tampa, FL, USA, Mar. 2017, pp. 1097–1102.
- [28] S. Vazquez, J. I. Leon, L. G. Franquelo, J. M. Carrasco, O. Martínez, J. Rodríguez, P. Cortes, and S. Kouro, "Model predictive control with constant switching frequency using a discrete space vector modulation with virtual state vectors," in *Proc. IEEE Int. Conf. Ind. Technol.*, Gippsland, VIC, Australia, Feb. 2009, pp. 1–6.
- [29] L.-H. Kim, J.-H. Kim, N.-K. Hahm, C.-Y. Won, and Y.-R. Kim, "A novel PWM switching technique for conducted EMI reduction in field-oriented control of an induction motor drive system," in *Proc. 31st Annu. Conf. IEEE Ind. Electron. Soc. (IECON)*, Raleigh, NC, USA, Nov. 2005, p. 6.
- [30] F. Morel, X. Lin-Shi, J. Retif, B. Allard, and C. Buttay, "A comparative study of predictive current control schemes for a permanent-magnet synchronous machine drive," *IEEE Trans. Ind. Electron.*, vol. 56, no. 7, pp. 2715–2728, Jul. 2009.
- [31] S. Kwak and S. K. Mun, "Model predictive control methods to reduce common-mode voltage for three-phase voltage source inverters," *IEEE Trans. Power Electron.*, vol. 30, no. 9, pp. 5019–5035, Sep. 2015.
- [32] H. Gao, B. Wu, D. Xu, M. Pande, and R. P. Aguilera, "Common-mode-voltage-reduced model-predictive control scheme for current-source-converter-fed induction motor drives," *IEEE Trans. Power Electron.*, vol. 32, no. 6, pp. 4891–4904, Jun. 2017.
- [33] S. A. Davari, D. A. Khaburi, and R. Kennel, "An improved FCS-MPC algorithm for an induction motor with an imposed optimized weighting factor," *IEEE Trans. Power Electron.*, vol. 27, no. 3, pp. 1540–1551, Mar. 2012.
- [34] L. Guo, X. Zhang, S. Yang, Z. Xie, and R. Cao, "A model predictive control-based common-mode voltage suppression strategy for voltage-source inverter," *IEEE Trans. Ind. Electron.*, vol. 63, no. 10, pp. 6115–6125, Oct. 2016.
- [35] M. G. Judewicz, S. A. González, J. R. Fischer, J. F. Martínez, and D. O. Carrica, "Inverter-side current control of grid-connected voltage source inverters with LCL filter based on generalized predictive control," *IEEE J. Emerg. Sel. Topics Power Electron.*, vol. 6, no. 4, pp. 1732–1743, Dec. 2018.



TAO JIN (SM'19) was born in Hubei, China, in 1976. He received the B.S. and M.S. degrees from Yanshan University, in 1998 and 2001, respectively, and the Ph.D. degree in electrical engineering from Shanghai Jiao Tong University, in 2005, where he was a Postdoctoral Researcher, from 2005 to 2007. During this time, he was in charge of a research group in the biggest dry-type transformer company in Asia, Sunten Electrical Company Ltd., to develop new transformer technology for distribution grids. From 2008 to 2009, he was a Research Scientist with Virginia Tech, Blacksburg, USA, where he was involved in the design and testing of PMU technology and GPS/internet-based power system frequency monitoring networks. In 2010, he joined Imperial College London, U.K., as a European Union Marie Curie Research Fellow, where he was focused on electrical technologies related to smart grids. He is currently a Professor with the College of Electrical Engineering & Automation, Fuzhou University, China. He has published about 110 papers.

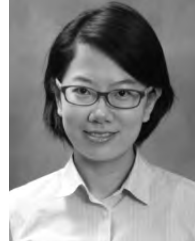
Prof. Jin is a member of the IEEE Power and Energy Society and the IEEE Industrial Electronics Society. He is also a special committee member of the Chinese Society of Electrical Engineering and the China Electro technical Society. He currently serves as an Associate Editor for the *China Measurement & Testing Technology* and other journals.



JINTAO GUO was born in Fujian, China, in 1995. He received the B.S degree from Fujian Agriculture and Forestry University, in 2017. He is currently pursuing the master's degree with the School of Electrical Engineering and Automation, Fuzhou University. His current research interests include model predictive control, and analysis and control for new energy grid-connected inverters.



MOHAMED A. MOHAMED was born in Minia, Egypt, in 1985. He received B.Sc. and M.Sc. degrees from Minia University, Minia, in 2006 and 2010, respectively, and the Ph.D. degree from King Saud University, Riyadh, Saudi Arabia, in 2016. He joined the College of Electrical Engineering & Automation, Fuzhou University, China, in 2018 as a Postdoctoral Research Fellow. He has been a Faculty Member with the Department of Electrical Engineering, College of Engineering, Minia University, since 2008. His current research interests include renewable energy, energy management, power electronics, power quality, optimization, and smart grids. He has supervised multiple M.Sc. and Ph.D. theses, worked on a number of technical projects, and published various papers and books. He has also joined the editorial board of some scientific journals and the steering committees of many international conferences.



MENGQI WANG (S'11–M'15) received the B.S. degree in electrical engineering from Xi'an Jiaotong University, Xi'an, China, in 2009, and the Ph.D. degree in electrical engineering from North Carolina State University, Raleigh, NC, USA, in 2014. Since 2015, she has been an Assistant Professor with the Department of Electrical and Computer Engineering, University of Michigan–Dearborn, Dearborn, MI, USA. Her research interests include power and energy systems, high efficiency and high-power density power supplies, renewable energy systems, and wide-bandgap power device application.

• • •